Journal of Zhejiang University SCIENCE
ISSN 1009-3095
http://www.zju.edu.cn/jzus
E-mail: jzus@zju.edu.cn

Use of 3-D magnetic resonance electrical impedance tomography in detecting human cerebral stroke: a simulation study*

GAO Nuo (高 诺)†1, ZHU Shan-an (朱善安)[1], HE Bin (贺 斌)†2

([1]*School of Electrical Engineering, Zhejiang University, Hangzhou 310027, China*)

([2]*Department of Biomedical Engineering, University of Minnesota, MN, USA*)

†E-mail: gaonuo@jnnc.com; binhe@umn.edu

Received Nov. 21, 2004; revision accepted Jan. 21, 2005

Abstract: We have developed a new three dimensional (3-D) conductivity imaging approach and have used it to detect human brain conductivity changes corresponding to acute cerebral stroke. The proposed Magnetic Resonance Electrical Impedance Tomography (MREIT) approach is based on the J-Substitution algorithm and is expanded to imaging 3-D subject conductivity distribution changes. Computer simulation studies have been conducted to evaluate the present MREIT imaging approach. Simulations of both types of cerebral stroke, hemorrhagic stroke and ischemic stroke, were performed on a four-sphere head model. Simulation results showed that the correlation coefficient (CC) and relative error (RE) between target and estimated conductivity distributions were 0.9245±0.0068 and 8.9997%±0.0084%, for hemorrhagic stroke, and 0.6748±0.0197 and 8.8986%±0.0089%, for ischemic stroke, when the SNR (signal-to-noise radio) of added GWN (Gaussian White Noise) was 40. The convergence characteristic was also evaluated according to the changes of CC and RE with different iteration numbers. The CC increases and RE decreases monotonously with the increasing number of iterations. The present simulation results show the feasibility of the proposed 3-D MREIT approach in hemorrhagic and ischemic stroke detection and suggest that the method may become a useful alternative in clinical diagnosis of acute cerebral stroke in humans.

Key words: Magnetic Resonance Electrical Impedance Tomography, Conductivity, Acute cerebral stroke, Hemorrhagic stroke, Ischemic stroke, Current density imaging

doi:10.1631/jzus.2005.B0438 **Document code:** A **CLC number:** TM153

INTRODUCTION

Magnetic Resonance Electrical Impedance Tomography (MREIT) is a new imaging technique combining traditional Electrical Impedance Tomography (EIT) and Current Density Imaging (CDI) for determining conductivity distribution inside a subject (Khang *et al*., 2002; Kwon *et al*., 2002). In MREIT, a current is injected into the subject through a pair of surface electrodes. The induced magnetic flux density inside the subject can be measured through a Magnetic Resonance Imaging (MRI) scanner (Pešikan *et al*., 1990; Scott *et al*., 1991; İder and Muftuler, 1997; Eyüboğlu *et al*., 1998) and the current density distribution can be calculated according to Ampere's law. Then the conductivity distribution images can be obtained through the relationship between the conductivity and the current density or the magnetic flux density (Birgül and İder, 1996; İder and Birgül, 1998; Khang *et al*., 2002; Kwon *et al*., 2002).

MREIT has been used for imaging absolute conductivity distribution and the results are encouraging (Khang *et al*., 2002; Kwon *et al*., 2002; Gao *et al*., 2004). In the present study, we use the MREIT technique to detect human brain conductivity changes.

It is well known that brain activity under some physiological phenomena will cause local and tem-

* Project supported partly by the National Science Foundation (No. BES-0411898) and the National Institues of Health (No. R01 EB00178), USA

poral conductivity changes within human brain tissue (Boone *et al*., 1997). Classical examples are the visual and auditory stimulations, migraines, strokes and epilepsy (Boone *et al*., 1994; Holder *et al*., 1999; Sadleir and Fox, 2001; Towers *et al*., 2000). Although the effects of these conditions vary in their magnitude and duration, each one tends to affect a particular area of the brain. This paper focuses on the brain conductivity changes due to acute cerebral strokes.

In the present study, we consider both types of acute cerebral stroke: ischemia and haemorrhage. Ischemia occurs when blood flow is reduced, e.g., due to a clogged artery. The most common technique for imaging stroke is MRI. However, while conventional MRI shows infracted (dead) tissue many hours after the onset of a stroke, it cannot readily detect ischemic tissue in the acute time window (i.e., within three hours), within which the tissue may be rescued by drug intervention.

Ischemic tissue is characterized by abnormally high impedance which occurs because of cell swelling that reduces the extracellular space and increases the bulk tissue impedance as much as 50% (Hansen and Olsen, 1989; Holder, 1992). The present work was motivated in part by the recognition that the reconstruction accuracy of MREIT is much better than that of traditional EIT and therefore we hypothesize that it may provide the sensitivity needed to detect conductivity changes caused by ischemia.

A related problem is hemorrhagic stroke, which occurs when blood fills the extracellular space or displaces brain tissue entirely. While far fewer patients have hemorrhagic stroke, it is much more likely to result in death. Ironically, the primary drug used to treat cerebral ischemia (t-PA) carries a 6% chance of causing brain hemorrhage (Albers *et al*., 1998). Since the conductivity of blood (σ_k=0.61 s/m) (Geddes and Baker, 1967) is approximately three times that of the brain, it seems reasonable to hypothesize that MREIT may be able to detect hemorrhagic stroke as well.

MREIT for the head is obviously handicapped by the low skull conductivity, since much of the current is shunted through the scalp and does not enter the brain compartment. Nevertheless, the reconstruction accuracy of MREIT is the same through the imaging space and the inner part of it will not blur, which will occur in traditional EIT (Khang *et al*., 2002; Kwon *et al*., 2002). In the present work, we conducted computer simulations to investigate how well can MREIT detect ischemic and hemorrhagic strokes in humans.

Three aspects of the present approach have direct bearing on the results. First, we assume that head geometry is known, since this data can be obtained from the MRI scanner. Second, we assume the current density distribution is known and this can be obtained through CDI. Third, to focus on the changes in brain conductivity which might occur in stroke, we fix the conductivity of the outer head tissues [scalp, skull and cerebrospinal fluid (CSF)] to their base values.

METHODS

Overview of the MREIT approach

The whole procedure of the proposed MREIT reconstruction approach is illustrated in Fig.1. A three-dimensional (3-D) head model was constructed based on structure MRI scans. In the present study, to demonstrate the feasibility of this MREIT approach, a simple four-sphere head model (Burger and Milaan, 1943; Geddes and Baker, 1967; Baumann *et al*., 1997) was used and we assumed uniform and isotropic conductivity for each sphere.

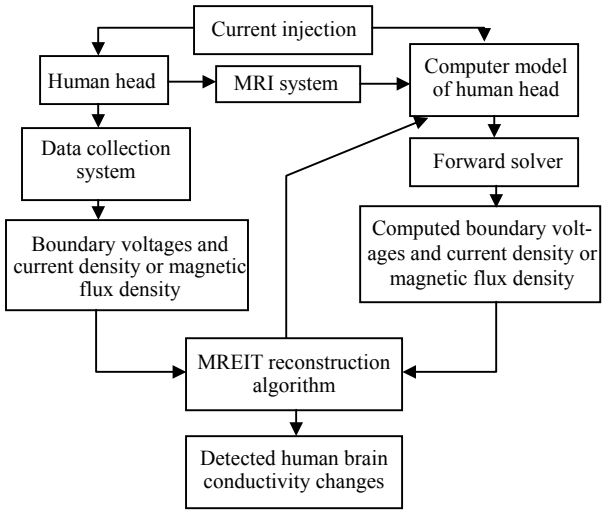

Fig.1 Schematic diagram of the present 3-D MREIT aproach

A current presumably of 100 μA was assumed to be injected into the human head through a pair of surface electrodes. A current under this limit is considered to be safe for human and would not elicit

neural activity (Clay and Ferree, 2002). The induced magnetic flux density can be measured by an MRI scanner and the current density distribution can be obtained. The present MREIT algorithm needs not only the current density distribution but also voltage differences between the two injection electrodes (Khang *et al*., 2002; Kwon *et al*., 2002; İder *et al*., 2003). In the present simulation study, the "measured" current density and voltage differences were simulated (Given the target conductivity distribution, through solving the forward problem, we can get the target current density and voltage differences. Different signal-to-noise ratio (SNR) Gaussian White Noise (GWN) was added to the target current density and voltage differences to simulate the "measured" noise-contaminated current density and voltage differences).

To assure the uniqueness of the results, three currents were assumed to be injected into the 3-D human head from three vertical directions (Khang *et al*., 2002; Kwon *et al*., 2002; İder *et al*., 2003) to obtain three "measured" current densities and voltage differences. The conductivity distribution is estimated by minimizing the differences between the "measured" and calculated current densities and voltage differences.

In the present study, we used an iterative algorithm called J-Substitution algorithm to update the conductivity change distribution. J-Substitution algorithm has been used to reconstruct 2-D subject absolute conductivity image (Khang *et al*., 2002; Kwon *et al*., 2002). Here, we extended it to reconstruct 3-D subject conductivity image and used it to detect human brain conductivity changes. To our knowledge, J-Substitution algorithm had not been applied previously for detecting human head conductivity changes.

In practical reconstruction procedure, since the target conductivity changes are unknown, we stop the iterative procedure when the difference of the two estimated conductivity changes is less than the allowable error. The mathematical model of the stopping criterion can be represented as follows:

$$\left\| \sigma^{i+1} - \sigma^{i} \right\| < \varepsilon \tag{1}$$

where σ^{i+1} represents the reconstructed conductivity distribution of the brain at the (i+1)th iteration and σ^{i} for the ith iteration. $\|\cdot\|$ is the Euclidian norm and ε is the allowable error. The selection of ε will affect the reconstruction accuracy and the convergence rate of the MREIT algorithm. The smaller the ε is, the higher the reconstruction accuracy is and the slower the convergence is.

Forward solver

Low frequency (f<10 kHz) current injected into the scalp creates quasistatic electric fields, which may be computed using techniques from electrostatics. For a good approximation, the electric and magnetic fields are decoupled and the local impedance is real.

With these simplifications, electric current in the conductive media is governed by Poisson's equation for the electric potential $U(r)$ subject to Neumann boundary conditions:

$$\nabla[\sigma(r)\nabla U(r)] = 0, \quad r \in \Omega \tag{2}$$

$$\sigma(\partial U/\partial n) = \begin{cases} J & \text{for positive current electrode} \\ -J & \text{for negative current electrode} \\ 0 & \text{elsewhere} \end{cases} \tag{3}$$

where $U(r)$ is the electric potential distribution, $\sigma(r)$ the conductivity distribution and Ω the subject to be imaged.

Analytical solutions for complex conductivity distribution are not available for the Neumann boundary value problem (NBVP) given by Eq.(2) and Eq.(3). Finite element method (FEM) was used to solve this NBVP. In the present study, we used ANSYS 8.1, a general-purpose finite element analytical software for the finite element modeling and analytical procedure.

After obtaining the electric potential distribution $U(r)$, the electric field $\vec{E}$ and current density distribution $\vec{J}$ can be calculated as:

$$\vec{E} = -\nabla U \tag{4}$$

$$\vec{J} = \sigma \vec{E} \tag{5}$$

Iterative reconstruction algorithm

Through solving the above forward problem, given a conductivity distribution σ, we can get a current density distribution J, and if the conductivity distribution is equal to the target conductivity σ^{*}, then the current density must be equal to the "measured"

current density J^*. According to the relationship between current density $\vec{J}$ and electric field $\vec{E}$, we define the objective function as:

$$f(\sigma)=\| |J^*|-\sigma\cdot|E| \| \quad (6)$$

Since σ is a scalar, we used the magnitude of the current density and electric field. $|J^*|$ is the magnitude of "measured" current density and $|E|$ is the magnitude of the calculated electric field when the conductivity is σ.

Minimizing the above objective function, we can get the update formula:

$$\sigma=|J^*|/|E| \quad (7)$$

To assure the uniqueness of the solution, the voltage differences between the injection electrodes must be added into the above update formula (Khang *et al*., 2002; Kwon *et al*., 2002; İder *et al*., 2003):

$$\sigma=(|J^*|/|E|)\times(V_\sigma/V_{\sigma^*}) \quad (8)$$

where V_σ is the calculated voltage difference when the conductivity is σ and V_{σ^*} is the "measured" voltage difference.

Simulation protocols

As mentioned above, we used a four-sphere head model and assumed uniform and isotropic conductivity for each sphere. The four spheres are brain, cerebrospinal fluid (CSF), skull and scalp, each characterized by a scalar conductivity σ and an outer radii r. The four spheres have outer radii (conductivities) of 8 cm (0.25 s/m) for the brain, 8.2 cm (1.79 s/m) for the CSF, 8.7 cm (0.018 s/m) for the skull and 9.2 cm (0.44 s/m) for the scalp (Burger and Milaan, 1943; Geddes and Baker, 1967; Baumann *et al*., 1997). The parameters of the four-sphere head model are listed in Table 1. Fig.2 shows the finite element (FE) mesh used for the simulations. It includes 35429 nodes and 25411 triangular elements.

Table 1 Head model parameters

	Brain	CSF	Skull	Scalp
r (cm)	8.0	8.2	8.7	9.2
σ (s/m)	0.25	1.79	0.018	0.44

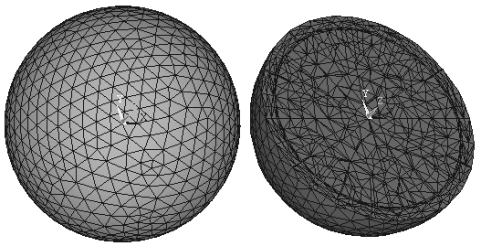

Fig.2 Finite element mesh for the four-sphere head model

To mimic the conductivity changes related to ischemic and hemorrhagic strokes, we used three focal anomalies that were located at three different locations. The three anomalies are numbered in order of decreasing depth. The first anomaly was in the center of the brain and the other two were shifted 3 cm in the brain radially along the x axis. Eighty-eight percents of ischemic and hemorrhagic strokes are of medium size (10–50 cm^3) (Reimann *et al*., 2000). In the present simulation, we set the volume of the three anomalies to be about 50 cm^3, which is about 2.3% of the brain. Anomaly 1 is comprised of 295 finite elements, anomaly 2 has 299 finite elements, and anomaly 3 consisted of 357 finite elements. The locations and volumes of the three anomalies are shown in Fig.3.

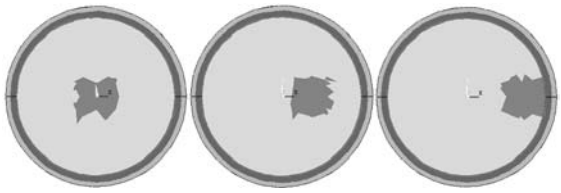

Fig.3 Illustration of locations and volumes of anomaly simulated

We assume that ischemic tissue may be characterized by a contiguous region with its conductivity equal to 50% of that of the brain: σ_i=0.125 s/m (Holder, 1992). We also assume that a hemorrhage may be characterized by a contiguous region with conductivity equal to that of blood: σ_h=0.61 s/m (Geddes and Baker, 1967). This assumes that blood completely displaces brain tissue, which is most common. It probably does not apply to the case where blood replaces only the extracellular fluid, which would tend to decrease the bulk tissue conductivity, since blood has lower conductivity than that of extracellular fluid.

To study the noise tolerance of the proposed

algorithm, different SNR GWNs were added to the target current density to simulate the "measured" noise contaminated J^*. The SNRs of GWN were infinite, 80, 60, 40, 20 and 10.

In the present study, the correlation coefficient (CC) and the relative error (RE) were used to quantitatively assess the performance of the MREIT reconstruction approach. The CC and RE between the target and estimated conductivity distribution are defined as follows:

$$CC[\sigma(n),\sigma^*(n)]=\frac{\sum_{n=1}^{N}\sigma(n)\cdot\sigma^*(n)}{\left[\sum_{n=1}^{N}\sigma^2(n)\right]^{1/2}\cdot\left[\sum_{n=1}^{N}\sigma^{*2}(n)\right]^{1/2}} \quad (9)$$

$$RE(\%)=(\|\sigma^*-\sigma\|/\|\sigma^*\|)\times 100\% \quad (10)$$

where σ^* is the target conductivity distribution and σ the estimated conductivity distribution.

In this study, we calculated CC and RE only within the brain region because we fixed the conductivity of the outer head tissues [scalp, skull and CSF] to their base values during our reconstruction procedure, so it is meaningless to calculate CC and RE for outer head tissues.

RESULTS

Reconstructed conductivity changes correspond to hemorrhagic stroke

The performance of this MREIT technique was tested by "simulated" hemorrhagic stroke with six noise levels. The three anomaly conductivities increase from brain conductivity (σ_b=2.5 s/m) to blood conductivity (σ_h=0.61 s/m). In each situation, different SNR of GWN was added to the target current density to simulate the "measured" current density. The simulation results are listed in Table 2.

The listed results in Table 2 show that the MREIT technique can detect the conductivity changes correspond to hemorrhagic stroke clearly. When there is no added GWN, all the CCs are nearly 1 and all the REs are less than 0.12% for the three anomalies. When the SNR of added GWN is 10, the CCs are all above 0.8 and REs are all less than 15%. Averaging all the three anomalies, the CC is 0.8383±0.0125 and the RE is 14.0111%±0.0538% when the SNR of the added GWN is 10. These promising results demonstrate the excellent detection ability of the proposed MREIT technique.

In Table 2 we also can see that when the SNRs of added GWN are the same, CC and RE change little among these three anomalies. This phenomenon shows that the spatial resolution of this technique is not affected by the location. This is quite different compared with traditional EIT technique. Traditional EIT's spatial resolution for the inner part is much lower than that of the outer part.

Fig.4 depicts the section map of the estimated results. In order to display the conductivity changes clearly, when we plot the section map, we set the conductivities of outer head tissues [scalp, CSF, skull] to be the same as the brain conductivity (they were all fixed to their base value when we conducted the simulation study).

In Fig.4, the left column corresponds to anomaly 1, the middle column corresponds to anomaly 2 and the right column corresponds to anomaly 3. The first row is the target conductivity distribution and the second to fifth rows correspond to the estimated results when the SNRs of added GWN are infinite, 80, 40 and 10, respectively. Fig.4 shows that these three

Table 2 Reconstructed results for hemorrhagic situation of three anomalies

Anomaly	*CC*/*RE*	SNR of added GWN					
		Infinite	80	60	40	20	10
1	*CC*	0.9999	0.9795	0.9545	0.9193	0.8859	0.8314
	RE (%)	0.1155	4.3830	6.6921	8.9906	11.3496	13.9800
2	*CC*	0.9999	0.9791	0.9543	0.9220	0.8823	0.8308
	RE (%)	0.0929	4.4224	6.7187	9.0012	11.4580	14.0732
3	*CC*	0.9999	0.9816	0.9603	0.9322	0.8930	0.8528
	RE (%)	0.0638	4.4479	6.6809	9.0072	11.5436	13.9800
Average	*CC*	0.9999±0.0000	0.9801±0.0013	0.9564±0.0034	0.9245±0.0068	0.8871±0.0054	0.8383±0.0125
	RE (%)	0.0907±0.0259	4.4178±0.0327	6.6972±0.0194	8.9997±0.0084	11.4504±0.0972	14.0111±0.0538

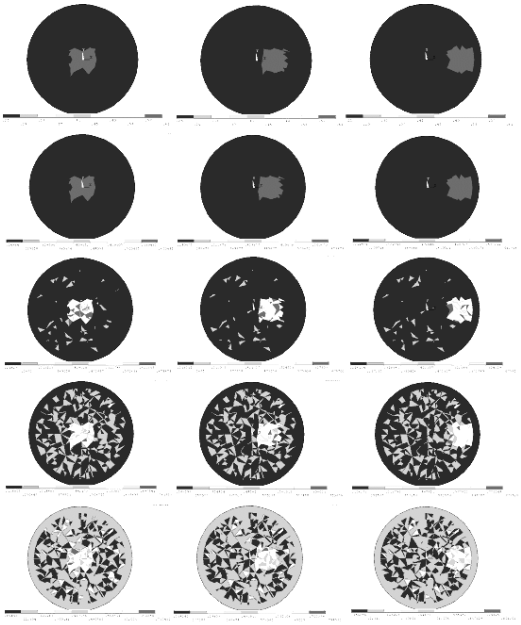

Fig.4 Reconstructed results for hemorrhage situation with different noise levels. The first row is the target conductivity distribution for three anomalies. The second to fifth row correspond to reconstructed results when the SNRs of added GWN are infinite, 80, 40 and 10

anomalies can be detected clearly by this MREIT technique even with high noise disturbance. This MREIT technique captures well the target conductivity distribution.

Fig.5 illustrates the CC values between target and estimated conductivity under different noise levels. Fig.5 indicates that with the increase of noise, the CC decreases monotonously. When the SNR of added GWN is 10, the CC is 0.8383±0.0125, which illuminates that a good estimation of the hemorrhagic stroke can be obtained with high noise disturbance.

Reconstructed conductivity distribution for ischemic stroke

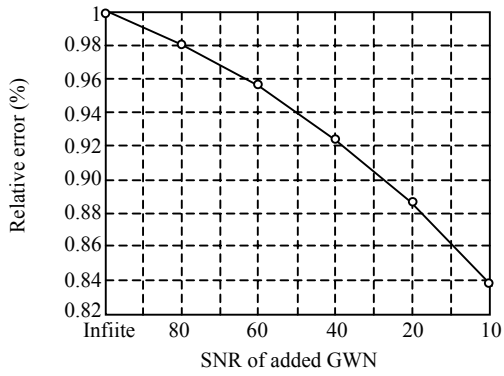

Fig.5 CC of averaged three anomalies of hemorrhage situation for six noise levels

The performance of the MREIT imaging approach was also evaluated by simulating ischemic stroke. All the simulation situations were the same as that of the hemorrhagic stroke except the magnitude of the conductivity changes. In ischemic stroke, we assume three anomaly conductivities to be 0.125 s/m, 50% of the brain. The magnitude of conductivity changes is much smaller than that of hemorrhagic stroke, so it is more difficult to detect ischemic stroke.

Fig.6 shows the reconstructed results for ischemic stroke, with the same display format as in Fig.4. The CC and RE for ischemic stroke are listed in Table 3, with the same format of Table 2. Averaging all three anomalies, the CC for the six noise levels are 0.9999±0.0000, 0.8786±0.0109, 0.7746±0.0173, 0.6748±0.0197, 0.5828±0.0230 and 0.5109±0.0175. The averaged RE with six noise levels are 0.0161%±0.0094%, 4.4144%±0.0091%, 6.6619%±0.0053%, 8.8986%±0.0089%, 11.4250%±0.0273% and 13.9051%±0.0100%. The promising results suggest the feasibility of the proposed MREIT technique in imaging human brain conductivity changes for ischemic stroke.

Table 3 Reconstructed results for ischemic situation of three anomalies

Anomaly	*CC*/*RE*	SNR of added GWN					
		Infinite	80	60	40	20	10
1	*CC*	0.9999	0.8711	0.7646	0.6672	0.5695	0.4989
	RE (%)	0.0245	4.4232	6.6649	8.9073	11.4407	13.9163
2	*CC*	0.9999	0.8735	0.7646	0.6601	0.5695	0.5029
	RE (%)	0.0179	4.4148	6.6649	8.8989	11.4407	13.8972
3	*CC*	0.9999	0.8911	0.7945	0.6972	0.6093	0.5310
	RE (%)	0.0060	4.4051	6.6558	8.8895	11.3935	13.9017
Average	*CC*	0.9999±0.0000	0.8786±0.0109	0.7746±0.0173	0.6748±0.0197	0.5828±0.0230	0.5109±0.0175
	RE (%)	0.0161±0.0094	4.4144±0.0091	6.6619±0.0053	8.8986±0.0089	11.4250±0.0273	13.9051±0.0100

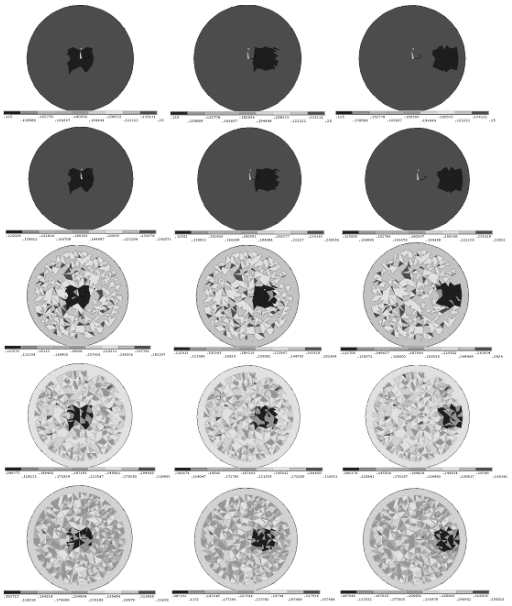

Fig.6 Reconstructed results for ischemic situation with different noise levels. The first row is the target conductivity distribution for three anomalies. The second to fifth row correspond to the reconstructed results when the SNRs of added GWN are infinite, 80, 40 and 10

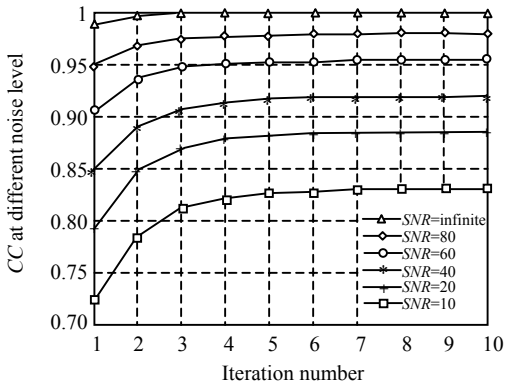

Fig.7 CC changes with iteration number of different noise level for hemorrhage situation of anomaly one

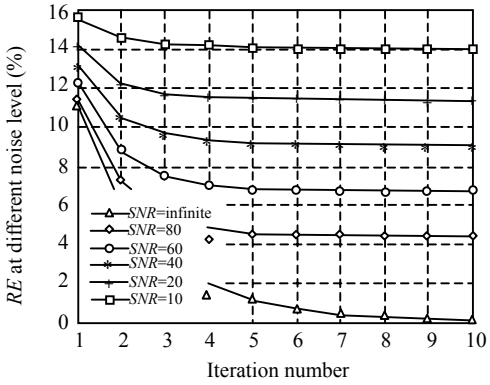

Fig.8 RE changes with iteration number of different noise level for hemorrhage situation of anomaly one

Convergence of the MREIT technique

In order to evaluate the convergence of the proposed MREIT technique, we study the changes of CC and RE. Fig.7 depicts the changes of CC for different iteration numbers for the hemorrhagic situation of anomaly 1. Fig.8 depicts the changes of RE for the same situation as Fig.7. Both Figs.7 and 8 include six curves corresponding to six noise levels.

In Fig.7, all six curves are monotonously increasing and in Fig.8, all curves are monotonously decreasing, suggesting good convergence characteristics of this technique. Similar trends were also observed for other two anomalies of hemorrhagic situation and three anomalies of ischemic situation.

DISCUSSION

In the present study, we have developed a new 3-D MREIT approach for noninvasive human brain conductivity change imaging. The proposed approach is based on the J-Substitution algorithm (Khang *et al*., 2002; Kwon *et al*., 2002) and is extended to 3-D subject conductivity imaging. To our knowledge, this is the first time that this approach is used to detect human brain conductivity changes.

The present study suggests that one can noninvasively estimate the location, size and magnitude of hemorrhagic and ischemic strokes with high accuracy and spatial resolution. For hemorrhagic situation, averaging three anomalies, the CC and RE between the target and estimated conductivity distribution were 0.9245±0.0068 and 8.9997%±0.0084%, when the SNR of added GWN was 40. For ischemic situation, averaging three anomalies, the CC and RE were 0.6748±0.0197 and 8.8986%±0.0089%, when the SNR of added GWN is 40. The present simulation results demonstrate the excellent performance of the proposed 3-D MREIT approach for imaging human brain conductivity changes.

Note that a four-sphere head model with isotropic nature was used in this study to represent the human head. A more sophisticated head model, e.g. real geometry head model with anisotropy nature, will enhance the accuracy and resolution of this approach. These works will be done in our future study.

In summary, we have developed a novel con-

ductivity imaging approach for noninvasive imaging of human brain conductivity changes caused by stroke. We have demonstrated, by computer simulations, the feasibility of the 3-D MREIT approach to estimate the location, size and magnitude of the stroke. Future investigation should also include in-depth examination of the effects of geometry error on imaging accuracy, location, volume and magnitude of the anomaly that can be detected and the experimental validation of this imaging approach in an experimental and clinical setting.

References

Albers, G.W., Easton, J.D., Sacco, R.L., Teal, P., 1998. Antithrombotic and thrombolytic therapy for ischemic stroke. *Chest*, **114**:683S-698S.

Baumann, S.B., Wozny, D.R., Kelly, S.K., Meno, F.M., 1997. The electrical conductivity of human cerebrospinal fluid at body temperature. *IEEE Transactions on Biomedical Engineering*, **44**:220-223.

Birgül, Ö., İder, Y.Z., 1996. Electrical Impedance Tomography Using the Magnetic Field Generated by Injected Currents. 18th Annual International Conference of the IEEE Engineering in Medicine and Biology Society, Amsterdam, p.784-785.

Boone, K., Lewis, A.M., Holder, D.S., 1994. Imaging of cortical spreading depression by EIT: Implictions for localization of epileptic foci. *Physiol Meas*, **15**(6):A189-A198.

Boone, K.G., Barber, D., Brown, B., 1997. Review imaging with electricity: Report on the European concerted action on impedance tomography. *Medical Engineering Technology*, **21**(6):201-232.

Burger, H.C., Milaan, J.B.V., 1943. Measurements of the specific resistance of the human body to direct current. *Acta Med. Scand*, **114**:584-607.

Clay, M.T., Ferree, T.C., 2002. Weighted regularization in electrical impedance tomography with applications to acute cerebral stroke. *IEEE Transactions on Medical Imaging*, **21**(6):629-637.

Eyüboğlu, B.M., Reddy, R., Leigh, J.S., 1998. Imaging electrical current density using nuclear magnetic resonance. *ELEKTRİK*, **6**(3):201-214.

Gao, N., Zhu, S.A., He, B., 2004. On the Measurement of Conductivity Distribution of the Human Head Using Magnetic Resonance Electrical Impedance Tomography. Proceedings of the 26th International Conference of the IEEE EMBS. SanFrancisco, CA, USA, p.4443-4446.

Geddes, L.A., Baker, L.E., 1967. The specific resistance of biological materials: A compendium of data for the biomedical engineer and physiologist. *Med. Biol. Eng*, **5**:271-293.

Hansen, J.H., Olsen, C.E., 1989. Brain extracellular space during spreading depression and ischemia. *Acta. Physiol. Scand*, **108**:355-365.

Holder, D.S., 1992. Detection of cerebral ischemia in the anaesthetized rat by impedance measurement with scalp electrodes: Implications for noninvasive imaging of stroke by electrical impedance tomography. *Clin. Phys. Physiol. Meas*, **13**:63-76.

Holder, D.S., Gonzalez-Correa, C.A., Tidswell, T., Gibson, A., Cusick, G., Bayford, R.H., 1999. Assessment and calibration of a low-frequency system for electrical impedance tomography (EIT), optimized for use in imaging brain function in ambulant human subjects. *Proc NY Acad Sci*, **873**:512-519.

İder, Y.Z., Muftuler, L.T., 1997. Measurement of AC magnetic field distribution using magnetic resonance imaging. *IEEE Transactions on Medical Imaging*, **16**(5):617-622.

İder, Y.Z., Birgül, Ö., 1998. Use of the magnetic field generated by the internal distribution of injected currents for Electrical Impedance Tomography (MR-EIT). *ELEKTRİK*, **6**(3):215-225.

İder, Y.Z., Onart, S., Lionheart, W.R.B., 2003. Uniqueness and reconstruction in magnetic resonance-electrical impedance tomography (MR-EIT). *Physiol. Meas*., **24**:591-604.

Khang, H.S., Lee, B.I., Oh, S.H., Woo, E.J., Lee, S.Y., Cho, M.H., Kwon, O., Yoon, J.R., Seo, J.K., 2002. J-Substitutition algorithm in magnetic resonance electrical impedance tomography (MREIT): Phantom experiments for static resistivity images. *IEEE Transactions on Medical Imaging*, **21**(6):695-702.

Kwon, O., Woo, E.J., Yoon, J.R., Seo, J.K., 2002. Magnetic resonance electrical impedance tomography (MREIT): simulation study of J-Substitution algorithm. *IEEE Transactions on Biomedical Engineering*, **49**(2):160-167.

Pešikan, P., Joy, M.L.G., Scott, G.C., Henkelman, R.M., 1990. Two-dimensional current density imaging. *IEEE Trans. Instrumentation and Measurement*, **39**(6):1048-1053.

Reimann, M., Niehaus, L., Lehmann, R., 2000, Magnetic resonance imaging of hemorrhagic transformation in ischemic posterior infarction. *Rofo*., **172**(8):675-679.

Sadleir, R.J., Fox, R.A., 2001. Detection and quantification of intraperitoneal fluid using electrical impedance tomography. *IEEE Transactions on Biomedical Engineering*, **48**(4):484-491.

Scott, G.C., Joy, M.L.G., Armstrong, R.L., Henkelman, R.M., 1991. Measurement of nonuniform current density by magnetic resonance. *IEEE Transactions on Medical Imaging*, **10**(3):362-374.

Towers, C.M., McCann, H., Wang, M., Beatty, P.C., Pomfrett, C.J.D., Beck, M.S., 2000. 3D simulation of EIT for monitoring impedance variations within the human head. *Physiol Meas*, **21**:119-124.